$[(Zr_6B)Cl_{11-x}I_{2+x}]$ ($0 \le x \le 6$): A New Mixed-Halide Structure with Zigzag Chains of Clusters in Multiply Twinned Crystals

Martin Köckerling* and Johannes B. Willems

Institut für Synthesechemie, FB 6 - Festkörperchemie, Gerhard-Mercator-Universität, Lotharstrasse 1, D-47057 Duisburg, Germany

Paul D. Boyle

Department of Chemistry, North Carolina State University, Raleigh, North Carolina 27695-8204

Received November 23, 1999

The new $[(Zr_6B)Cl_{11-x}I_{2+x}]$ phase (with $0 \le x \le 6$) is obtained from reactions of ZrI_4, $ZrCl_4$, and elemental Zr and B for 2−4 weeks in sealed Ta tubing at 800−850 °C. Single crystals of $[(Zr_6B)Cl_{6.44(7)}I_{6.56}]$ have been characterized by X-ray diffraction at room temperature (orthorhombic *Pbcn*, $Z = 4$, $a = 12.365(2)$ Å, $b = 15.485(3)$ Å, $c = 13.405(2)$ Å). This structure contains zigzag chains of boron-centered (Zr_6B) octahedra that are interconnected by Cl^{i-i} halides. Further three-dimensional connectivity is achieved by I^{a-a-a} bridges. The noncluster interconnecting two-bonded X^i sites are occupied statistically by a mixture of Cl and I. For each site both positions were resolved. This structure forms within a phase width of $0 \le x \le 6$ at temperatures between 800 and 850 °C. Crystals of this phase appear to be always multiply twinned.

Introduction

The extraordinary richness of the cluster chemistry in the reduced zirconium halides is based on the intrinsic stability of Zr_6 octahedra. These metal octahedra are always centered by an interstitial stabilizer Z, which may be H, the second-period members Be through N, Al, Si, Ge, P, or the transition metals Cr through Ni.[1−3] All 12 edges of the metal octahedra are bridged by *inner* halide atoms X^i with additional halides X^a occupying the *outer*, exo positions.[5] The need for 14 (with a main group element interstitial) or 18 (with a transition metal element interstitial) cluster-based electrons[4] allows for several variables to be tuned, giving rise to more than 30 different structure types. Nearly all of these compounds fall within the formula type $A^{I,II}_x[(Zr_6Z)X^i_{12}X^a_n]$, with $A^{I,II}$ = group 1 or 2 cation, X = Cl, Br, or I, $0 \le x \le 6$, and $0 \le n \le 6$.[6] For zirconium chlorides and bromides, the largest variety of different structure types is found for all $0 \le x, n \le 6$. In contrast, zirconium iodides are so far only known for the $[(Zr_6Z)I_{12}]$ ($n = 0$) and $A^I[(Zr_6Z)I_{14}]$ ($n = 2$) families but with a larger variety of Z.

Investigations of bromides gave close relatives to their chloride counterparts as well as five new unprecedented structure types.[7−9] These findings illustrate how small variations in size and/or basicity of the anions can have a large effect on the stability of a specific cluster phase or structure with respect to other members of the series. This observation prompted research of mixed-halide zirconium systems, aiming for hitherto unknown structure types. One of the initial results of these investigations in the zirconium−chloride−iodide systems is that intercluster bridging halide positions are occupied solely by one halide type; only noncluster interconnecting positions (X^i) may have (statistical) mixed occupation.[10] The cubic structures of $Na[(Zr_6B)Cl_{12-x}I_{2+x}]$ (with $x \le 6$) and $A^{II}[(Zr_6B)Cl_{12-x}I_{2+x}]_2$ (with A^{II} = Ca, Sr, Ba) were reported recently.[11,12]

In some of the reaction products of these investigations an unknown phase was obtained, named "unknown A" in refs 10 and 12. Guinier powder patterns of this material show this phase to crystallize in a new structure type. This paper reports the chemistry and the novel structure of this phase, which turned out to be $[(Zr_6Z)Cl_{11-x}I_{2+x}]$ (with $0 \le x \le 6$ for Z = B).

Experimental Section

Materials. The preparation and handling of the air- and moisture-sensitive reactants as well as of the reaction products, the use of sealed tantalum ampules, and the phase identification and yield estimation by means of Guinier powder patterns have been described previously.[12] The zirconium used was either from Ames Lab (reactor-grade crystal bar, <500 ppm of Hf) or from Strem (99.5%, *Hf-free*). Aldrich was the supplier of beryllium (99.9%), $ZrCl_4$ (99.5%, <50 ppm of Hf), and boron (amorphous, 99.999%).

Caution! The handling of beryllium and beryllium compounds involves hazards because they are severe poisons and have the ability to cause cancer!

ZrI_4 was prepared and purified by standard procedures according to ref 13. $MgCl_2$ was prepared by dissolving elemental Mg (Strem, 99.9%) in HCl, evaporating the resulting solution to dryness, and heating the white material at 550 °C under high vacuum for several hours. $LaCl_3$

(1) Ziebarth, R. P.; Corbett, J. D. *Acc. Chem. Res.* **1989**, *22*, 256.
(2) Corbett, J. D. *J. Chem. Soc., Dalton Trans.* **1996**, 575.
(3) Corbett, J. D. In *Modern Perspectives in Inorganic Crystal Chemistry*; Parthé, Ed.; Kluwer: Dordrecht, The Netherlands, 1992; p 27.
(4) Hughbanks, T.; Rosenthal, G.; Corbett, J. D. *J. Am. Chem. Soc.* **1988**, *110*, 1511.
(5) Schäfer, H.; von Schnering, H.-G. *Angew. Chem.* **1964**, *76*, 833.
(6) A more complicated cation/anion combination is found in $(Cs^+)_3[ZrCl_5]^-[(Zr_6Mn)Cl_{15}]^{2-}$. Zhang, J.; Corbett, J. D. *Inorg. Chem.* **1995**, *34*, 1652.
(7) Qi, R.-Y. Ph.D. Dissertation, Iowa State University, Ames, IA, 1993.
(8) Qi, R.-Y.; Corbett, J. D. *Inorg. Chem.* **1995**, *34*, 1646.
(9) Qi, R.-Y.; Corbett, J. D. *Inorg. Chem.* **1995**, *34*, 1657.
(10) Köckerling, M.; Qi, R.-Y.; Corbett, J. D. *Inorg. Chem.* **1996**, *35*, 1437.
(11) Köckerling, M. *Inorg. Chem.* **1998**, *37*, 380.
(12) Köckerling, M. *Z. Anorg. Allg. Chem.* **1999**, *625*, 24.
(13) Daake, R. L.; Corbett, J. D. *Inorg. Synth.* **1983**, *22*, 26.

10.1021/ic991359v CCC: $20.00
Published on Web 03/02/2001

Table 1. Details of Different Reactions Aiming for the $[(Zr_6B)Cl_{11-x}I_{2+x}]$ Phase

reaction no.	loaded composition	I/Cl ratio	phases found	reaction temp (°C)	reaction time[a]
1	$Zr_6Cl_3I_{10}B$	3.33	$[(Zr_6B)Cl_xI_{12-x}]$ (>95%)	850	3 w
2	$Zr_6Cl_5I_8B$	1.6	$[(Zr_6B)Cl_xI_{12-x}]$ (75%), $[(Zr_6B)Cl_{11-x}I_{2+x}]$ (25%)	800	5 w
3	$Zr_6Cl_5I_8B$	1.6	$[(Zr_6B)Cl_{11-x}I_{2+x}]$ (>95%)	850	5 w
4	$Zr_6Cl_7I_7B$	1.0	$[(Zr_6B)Cl_{11-x}I_{2+x}]$ (>95%)	825	3 w
5	$Zr_6Cl_7I_7B$	1.0	$[(Zr_6B)Cl_{11-x}I_{2+x}]$ (>95%)	850	4 w
6	$Zr_6Cl_5I_5B$	1.0	$[(Zr_6B)Cl_{11-x}I_{2+x}]$ (>95%)	850	4 w
7	$Zr_6Cl_5I_3B$	0.6	$[(Zr_6B)Cl_{11-x}I_{2+x}]$ (70%), Zr (30%)	850	4 w
8	$Zr_6Cl_{10}I_4B$	0.4	$[(Zr_6B)Cl_{11-x}I_{2+x}]$ (>95%)	850	2.5 w
9	$Zr_6Cl_6I_2B$	0.33	$[(Zr_6B)Cl_{11-x}I_{2+x}]$ (90%), $Zr(Cl,I)B_x$ (10%)	800	3 w
10	$Zr_6Cl_7I_2B$	0.28	$[(Zr_6B)Cl_{11-x}I_{2+x}]$ (80%), $Zr_2(Cl,I)_2B$ (10%), Zr (10%)	800	3 w
11	Zr_6Cl_7IB	0.143	$[(Zr_6B)Cl_{13-x}I_x]$ (85%), $[(Zr_6B)Cl_{11-x}I_{2+x}]$ (15%)	825	3 w
12	Zr_6Cl_9IB	0.11	$[(Zr_6B)Cl_{13-x}I_x]$ (>95%)	850	4 w
13	Zr_6ClI_7	7.0	ZrI_3,$ZrCl_xI_{2+x}$	750	4 w
14	Zr_6I_8B		ZrI_3, $[(Zr_6B)I_{12}]$	700	3 w
15	$Zr_6Cl_5I_8B$	1.6	ZrI_3, $ZrCl_2$	700	5 w
16	$Zr_6Cl_5I_8B$	1.6	$[(Zr_6B)Cl_xI_{12-x}]$ (90%), $[(Zr_6B)Cl_{11-x}I_{2+x}]$ (10%)	750	5 w
17	$Zr_6Cl_5I_5B$	1.0	$[(Zr_6B)Cl_{11-x}I_{2+x}]$ (20%), $[(Zr_6B)Cl_{12-x}I_x]$ (80%)	750	1 w
18	$Mg(Zr_6Cl_{11}I_3B)_2$	0.09−0.33	$[(Zr_6B)Cl_{11-x}I_{2+x}]$, $Mg(Cl, I)_2$	850	4 w
19	$La(Zr_6Cl_{11}I_3B)_3$	0.3−0.375	$[(Zr_6B)Cl_{11-x}I_{2+x}]$, $LaCl_3$	850	4 w
20	$Zr_6Cl_6I_6Be$	1.0	$[(Zr_6Be)Cl_xI_{12-x}]$ (>95%)	775	12 d
21	Zr_6Cl_6IBe	0.143	$[(Zr_6Be)Cl_xI_{12-x}]$ (>95%)	800	2 w

[a] w = week. d = day.

was obtained by the "ammonium halide method" and purified by high-vacuum sublimations.[29]

Syntheses. Appropriate amounts of the starting materials (total of 250 mg) were loaded in acid-cleaned, thoroughly washed and dried Ta or Nb ampules that were arc-welded under an Ar atmosphere. Up to four metal ampules were sealed in silica jackets under high vacuum. These tubes were heated in tubular furnaces at temperatures between 750 and 850 °C for up to 5 weeks. After the samples were quenched at room temperature, the metal ampules were opened in a drybox (MBraun) under inert gas.

The powder pattern of the new $[(Zr_6Z)Cl_{11-x}I_{2+x}]$ (Z = B) phase was seen in the products of reactions with $ZrCl_4$, ZrI_4, Zr, and B as starting materials. Details about the different reactions, loaded compositions, temperatures, reaction times, and resulting phases are given in Table 1. From these reactions the phase width has been deduced. With cations present, this phase is not observed as long as the cations are part of the cluster phase, but rather the cubic $A_z^{I,II}[(Zr_6B)Cl_{12-x}I_{2+x}]$ structure ($0 \le x \le 6$, $z = 1$ for A^I = Na, $z = 0.5$ for A^{II} = Ca, Sr, Ba) forms.[10,11] Furthermore, with K-, Rb-, or Cs-containing starting materials a new $A_2[(Zr_6Z)(X,X')_{15}]$ structure (X = Cl, X′ = I, Z = B) is obtained.[14] With Mg or La present, apparently no cation-containing cluster phase is as stable as the new $[(Zr_6B)(X,X')_{13}]$ structure, which is formed in addition to simple Mg- or La-containing salts. Reactions loaded with interstitials other than B (like H, Be, C, N, ...) never gave the title phase under the chosen reaction conditions. Unit cell parameters of several members of the new $[(Zr_6B)Cl_{11-x}I_{2+x}]$ phase with different Cl to I ratios are listed in Table 2.

Table 2. Unit Cell Parameters and Volumes for the $[(Zr_6B)Cl_{11-x}I_{2+x}]$ Phase with Different I/Cl Ratios in the Starting Materials

loaded composition	I/Cl ratio	*a* (Å)	*b* (Å)	*c* (Å)	*V* (Å^3)
$Zr_6Cl_7I_2B$	0.29	12.051(4)	15.359(3)	12.593(2)	2331(1)
$Zr_6Cl_6I_2B$	0.33	12.080(4)	15.382(6)	12.552(6)	2332(2)
$Zr_6Cl_8I_3B$	0.37	12.238(4)	15.346(5)	13.254(7)	2439(2)
$Zr_6Cl_7I_7B$	1.0	12.311(1)	15.426(2)	13.324(2)	2530.3(6)
$Zr_6Cl_7I_7B$	1.0	12.331(4)	15.416(5)	13.381(4)	2544(1)
$Zr_6Cl_5I_5B$	1.0	12.365(2)	15.485(3)	13.405(2)	2566.7(8)
$Zr_6Cl_5I_5B$	1.0	12.328(2)	15.450(6)	13.361(2)	2550(1)
$Zr_6Cl_5I_8B$	1.6	12.354(3)	15.446(4)	13.373(3)	2552(1)

Powder X-ray Diffraction Studies. Phases within the reaction products were identified with the aid of Guinier powder patterns. They were taken using evacuable Enraf-Nonius FR552 cameras with the samples mounted between pieces of Scotch tape. Identification was done by comparison of the line distribution on the film with patterns calculated on the basis of single-crystal data of known structures. Phase yields were estimated visually from the patterns, with a detection limit of up to 5%. Lattice parameters were obtained by least-squares fits of the positions of indexed lines; elemental Si was added as the internal standard.[27,28]

Single-Crystal X-ray Diffraction Studies. Crystals of the $[(Zr_6B)Cl_{11-x}I_{2+x}]$ phase, which form large black blocks with well-developed faces, were sealed by flame in thin-walled capillaries ("Mark-Röhrchen") for all single-crystal X-ray diffraction experiments. At the beginning of the structure determination, lattice parameters of several crystals were checked by indexing reflections centered on four-circle diffractometers. They all gave trigonal cells with $a = b \approx 32$ Å, $c \approx 12.5$ Å. Data sets taken from these crystals had many weak reflections and some "noncrystallographic" extinctions. Structure solutions attempted in the space group $P\bar{3}$ could not be refined to $R(F)$ values below ~20% and suffered further from a very unequal distribution of the isotropic temperature factors of the atoms. Also, powder patterns calculated on the basis of this structural model did not match the experimental patterns. Therefore, a full sphere of data was taken on an

(14) Köckerling, M. Unpublished research.
(15) Ziebarth, R. P.; Corbett, J. D. *J. Am. Chem. Soc*. **1985**, *107*, 4571.
(16) It is important to note that this $\bar{3}$ symmetry element is only used to describe the positional relation between the two X^{i-i} atoms of each cluster. It is not present in the three-dimensional structure.
(17) Hughbanks, T.; Corbett, J. D. *Inorg. Chem*. **1989**, *28*, 631.
(18) Payne, M. W.; Corbett, J. D. *Inorg. Chem*. **1990**, *29*, 2246.
(19) Llusar, R.; Corbett, J. D. *Inorg. Chem*. **1994**, *33*, 849.
(20) Barbour, L. J. *LAYER*, version 1.04; University of Missouri: Columbia, MO, 1995.
(21) Sheldrick, G. M. *Shelx-97*. Programs for the Refinement of Crystal *Structures*; University of Göttingen: Göttingen, Germany, 1997.
(22) Park, Y.; Corbett, J. D. *Inorg. Chem*. **1994**, *33*, 1705.
(23) Lulei, M.; Martin, J. D.; Corbett, J. D. *J. Solid State Chem*. **1996**, *125*, 249.
(24) Simon, A.; Mattausch, Hj.; Miller, G. J.; Bauhofer, W.; Kremer, R. K. In *Handbook on the Physics and Chemistry of Rare Earths*; Gschneider, K. A.; Eyring, L., Eds.; Elsevier Science: Amsterdam, 1991; Vol. 15, p 191.
(25) Sägeblatt, M.; Simon, A. *Z. Anorg. Allg. Chem*. **1990**, *587*, 119.
(26) Duisenberg, A. J. M. DIRAX: Indexing in Single-Crystal Diffractometry with an Obstinate List of Reflections. *J. Appl. Crystallogr*. **1992**, *25*, 92.
(27) Smith, J. D.; Corbett, J. D. *J. Am. Chem. Soc*. **1985**, *107*, 5704.
(28) Daake, R. L.; Corbett, J. D. *Inorg. Chem*. **1978**, *17*, 1192.
(29) Meyer, G. *Inorg. Synth*. **1985**, *25*, 146.

Enraf-Nonius Kappa CCD diffractometer up to 45° in 2θ. These data did not show $\bar{3}$ or *mmm* (after axis transformation) Laue symmetry. An attempt to refine the structure satisfactorily in space group $P\bar{1}$ failed as well, giving results similar to those described above for space group $P\bar{3}$. At this point twinning (multiple crystals) was considered. From the diffraction vectors of randomly picked reflections from the CCD data set, the program DIRAX[26] suggested a primitive orthorhombic cell of the dimensions $a = 12.346$ Å, $b = 13.404$ Å, and $c = 15.478$ Å. Graphical inspection of different layers of the CCD data set (program LAYER[20]) showed that almost all of the reflections can be accounted for by a nonmerohedral trilling with three components of this orthorhombic cell, each rotated by 60° relative to the others. With this information the data set was reindexed and batch numbers for each component were added (HKLF 5 format, program ShelxL-97[21]). Because of overlapping peaks, systematic extinctions cannot be used for the space group determination. Starting from low-symmetry orthorhombic ones, the space group was finally established through the successful refinement to be *Pbcn* (No. 60). The trilled refinement of the structural model using the ShelxL-97 program,[21] described below, converged at R1 ≈ 10% with amounts of ~63%, ~32%, and ~5% for the three components. Inspection of the difference electron map showed that several larger peaks exist that could not be accounted for in a reasonable model. However, the calculated powder pattern obtained from the atomic parameters of this refinement matches the experimental pattern, confirming the principal correctness of the refined structure.

Since the refinement of the trilled model was not completed satisfactorily, another crystal that was a much smaller specimen than before was investigated. Twenty carefully centered reflections were indexed to the above-described orthorhombic cell with $a = 12.365(2)$ Å, $b = 15.485(3)$ Å, and $c = 13.405(2)$ Å. One hemisphere of data was collected up to 54° in 2θ on a Siemens P4 four-circle diffractometer at room temperature. To check for the existence of any further components, axial photographs were taken with long exposure times. These showed a few additional but very weak spots between the layers. Attempts to measure any of these using a conventional diffractometer showed that their intensities are only about a few $\sigma(I)$, even with slow scan rates (but see below). Thus, they were not taken into account at this stage. From the systematic absences and intensity statistics the space group *Pbcn* (No. 60) was uniquely determined, confirming the space group choice taken in the trilled model. The data reduction involved Lorentz and polarization corrections as well as an empirical absorption correction based on ψ-scans from three reflections. It should be noted that most absorption correction routines can only be used on one-component (single) crystals with known orientation. Since the final crystal structure determination of the title phase was done with data from a small crystal (even smaller than the optimum crystal size as estimated by $a \approx 3/\mu$; see ref 31) and on a specimen that consists largely of only one component with the twinning being accounted for by a disorder model (see below), an empirical absorption correction seems applicable. This choice is further supported by comparison of the refinement results with those using uncorrected data, which virtually give the same structural data but higher *R* values. Averaging the data in Laue group mmm gave $R_{int} = 1.7\%$. The atom positions that were derived from the trilled model were utilized as an initial model. After isotropic refinement, the inspection of the difference Fourier peaks showed the presence of a disordered iodine atom. Thus, the final refinement was done assuming a fully occupied halide sublattice in which the metal octahedra and one iodine atom are disordered on two positions. The final refinement accounted for the twinning as a disorder rather than an explicitly twinned structure. This was done because reflections from the minor twin were not included in the data set. (1) To see if such a procedure gives the correct structure and (2) to establish the origin of the weak reflections that were not taken into account so far, a complete data set was taken on a Bruker Smart-CCD diffractometer at room temperature. After indexing of the strong reflections in the three-component trilling, indexing of several hundred of the unassigned weak reflections gave the same trilling of orthorhombic cells but with a different orientation. Thus, crystals of this phase form six-component units arranged as twins of trilling of orthorhombic cells. Since such an arrangement cannot be handled by any of the available crystal structure refinement programs, the trilling refinement was performed on the larger part with the second twin of trillings being described by a disorder model as above. This resulted in the same structure as the one described above with very similar positional and thermal parameters but larger *R* values. Therefore, all further descriptions and discussions are based on the former refinement.

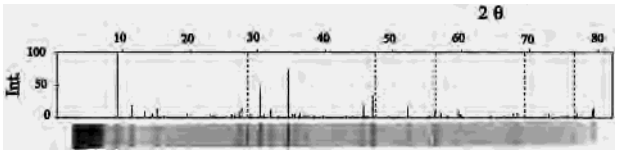

Figure 1. Comparison of the experimental Guinier pattern (bottom) with the line distribution (top) calculated using the refined atom position of $[(Zr_6B)Cl_{6.44(7)}I_{6.56}]$.

Table 3. Data Collection and Structure Determination Parameters for $[(Zr_6B)Cl_{6.44(7)}I_{6.56}]$

empirical formula	$Zr_6Cl_{6.44(7)}I_{6.56}B$
fw	1618.964
space group, *Z*	*Pbcn* (No. 60), 4
a [Å]	12.365(2)
b [Å]	15.485(3)
c [Å]	13.405(2)
V [Å^3]	2566.7(8)
d_{calcd} [g/cm^3]	4.189
temp [°C]	21
μ (Mo Kα) [cm^{-1}]	108.9
R1,[a,b] wR2[b]	0.0621, 0.1421

[a] For 1286 reflections with $F_o > 4\sigma(F_o)$. [b] $R1 = [\sum||F_o| - |F_c||]/\sum|F_o|$. $wR2 = \{[\sum w(F_o^2 - F_c^2)^2]/\sum w(F_o^2)^2\}^{1/2}$.

As found already for the other known mixed-halide (I, Cl) zirconium clusters,[10−12] the two-bonded X^i positions are substitutionally disordered. The fractional sites (I3 − I8 + Cl3 − Cl8) were positionally resolved in all cases with the sum of the occupancies being constrained to unity. Halide site ×2, which is located on an inversion center, is a chloride site with a small substitution of iodide (see below). The two fractional atoms were refined with the same anisotropic displacement parameters for both. In all cases the zirconium and iodine atoms were refined anisotropically and the Cl and B atoms isotropically. This model converged at R1 = 6.21% and wR2 = 14.21%. The largest peaks in the final difference Fourier map are +1.16 e/Å^3 (1.03 Å from I1) and −0.93 e/Å^3.

From the final atom coordinates a Guinier-type line pattern was calculated. The match with the experimental pattern is depicted in Figure 1. Some data collection and refinement parameters are given in Table 3. The final atomic positions and isotropic equivalent displacement parameters for the structure of the title phase, and their estimated standard deviations are listed in Table 4 and important distances in Table 5. Additional data collection and refinement information, the anisotropic displacement parameters, and full listings of atom distances are available as Supporting Information. The last plus the structure factor data are also available from M.K.

Chemical Analysis. To check for the correctness of the formula as derived from the single-crystal X-ray structure determination, i.e., for the chlorine-to-iodine ratio, a potentiometric halogen determination was performed. Selected representative crystals of the title phase (36.4 mg) were dissolved in 25 mL of 0.1 *m* NaOH solution and titrated using 0.01 *m* $AgNO_3$. The total halide content was determined to be 65.49%. With the assumption of 6 Zr atoms, 1 B atom, and a total of 13 halogen atoms per formula unit, a composition of $Zr_6Cl_{6.46(5)}I_{6.54}B$ was calculated, which agrees well with the halide distribution obtained from the X-ray analysis.

(30) Hong, S.-T.; Hoistad, L. M.; Corbett, J. D. *Inorg. Chem.* **2000**, *39*, 98.

(31) Giacovazzo, C.; Monaco, H. L.; Viterbo, D.; Scordari, F.; Gilli, G.; Zanotti, G.; Catti, M. In *Fundamentals of Crystallography*; Giacovazzo, C., Ed.; Oxford University Press: Oxford, U.K., 1992; pp 304−305.

Table 4. Positional and Isotropic Displacement Parameters for $[(Zr_6B)Cl_{6.44(7)}I_{6.56}]$

atom	wyckoff position	*x*	*y*	*z*	occupation[a]	U_{eq} [b]
			Main Component			
Zr1	8d	0.3910(2)	0.7313(1)	0.1782(1)	0.822(2)	0.0191(5)
Zr2	8d	0.3896(2)	0.5186(1)	0.1815(1)	0.822(2)	0.0192(5)
Zr3	8d	0.3900(2)	0.6271(1)	0.3915(1)	0.822(2)	0.0197(4)
I1	8d	0.2513(1)	0.87823(9)	0.08189(7)	1.0	0.0330(3)
I2	4a	0.5	0.5	0	0.291(8)	0.037(1)
Cl2	4a	0.5	0.5	0	0.709	0.037(1)
I3	4c	0.5	0.8845(5)	0.25	0.388(8)	0.032(2)
Cl3	4c	0.5	0.863(1)	0.25	0.612	0.034(7)
I4	8d	0.4992(7)	0.7527(5)	−0.0062(6)	0.432(6)	0.035(1)
Cl4	8d	0.501(2)	0.742(2)	0.012(2)	0.568	0.037(6)
I5	8d	0.2372(4)	0.6237(4)	0.0827(3)	0.478(7)	0.035(1)
Cl5	8d	0.269(1)	0.624(1)	0.090(1)	0.522	0.032(4)
I6	4c	0.5	0.369(2)	0.25	0.287(8)	0.032(3)
Cl6	4c	0.5	0.384(2)	0.25	0.713	0.04(1)
I7	8d	0.2393(4)	0.4993(3)	0.3363(4)	0.441(6)	0.036(1)
Cl7	8d	0.2706(10)	0.5049(9)	0.330(1)	0.559	0.025(3)
I8	8d	0.243(1)	0.7504(8)	0.3335(7)	0.444(6)	0.040(2)
Cl8	8d	0.256(4)	0.745(3)	0.323(2)	0.556	0.044(9)
B1	4c	0.5	0.626(2)	0.25	0.822(2)	0.022(6)
			Minor Component			
Zr1A	8d	0.1092(8)	0.5183(5)	0.1787(6)	0.178	0.021(2)
Zr2A	8d	0.1096(7)	0.6243(6)	0.3914(6)	0.178	0.024(2)
Zr3A	8d	0.1101(8)	0.7305(5)	0.1785(7)	0.178	0.024(2)
I9	4b	0	0.5	0	0.111(3)	0.051(3)

[a] The sum of the occupancies of each of the Zr atoms of both components were fixed to unity as well as the occupancy of each split halide position. [b] $U_{eq} = (1/3)\sum_i\sum_j u_{ij} a_i^* a_j^* \vec{a}_i \vec{a}_j$.

Table 5. Important Interatomic Distances (Å) for $[(Zr_6B)Cl_{6.44(7)}I_{6.36}]$ (Main Component)

Zr−Zr:			Zr−I^{a-a-a}:		
Zr1−Zr1		3.312(4)	Zr1−I1	×6	3.135(2)
Zr1−Zr2	x2	3.294(2)	Zr2−I1	×6	3.089(2)
Zr1−Zr3	x2	3.283(2)	Zr3−I1	×6	3.095(2)
	x2	3.288(3)			
Zr2−Zr2		3.290(4)	$\bar{d}$		3.106
Zr2−Zr3	x2	3.347(2)			
	x2	3.278(2)			
$\bar{d}$		3.299	Zr-$X2^{i-i}$:		
			Zr2−$I2^a$	×2	2.804(2)
Zr−B:			Zr3−$I2^a$	×2	2.800(2)
Zr1−B1	×2	2.33(2)	Zr2−$Cl2^a$	×2	2.804(2)
Zr2−B1	×2	2.34(2)	Zr3−$Cl2^a$	×2	2.800(2)
Zr3−B1	×2	2.334(2)	$\bar{d}$		2.802
$\bar{d}$		2.335			
Zr−I^i:			Zr−Cl^i:		
Zr1−$I3^b$	×2	2.893(7)	Zr1−$Cl3^b$	×2	2.62(3)
Zr1−$I4^c$		2.830(8)	Zr1−$Cl4^c$		2.62(2)
Zr3−$I4^c$		2.832(8)	Zr3−$Cl4^c$		2.58(2)
Zr1−$I5^d$		2.834(5)	Zr1−$Cl5^d$		2.54(2)
Zr2−$I5^d$		2.821(5)	Zr2−$Cl5^d$		2.53(2)
Zr2−$I6^e$	×2	2.85(2)	Zr2−$Cl6^e$	x2	2.66(3)
Zr2−$I7^f$		2.803(5)	Zr2−$Cl7^f$		2.48(1)
Zr3−$I7^f$		2.816(5)	Zr3−$Cl7^f$		2.54(1)
Zr1−$I8^g$		2.79(1)	Zr1−$Cl8^g$		2.57(4)
Zr3−$I8^g$		2.75(1)	Zr3−$Cl8^g$		2.63(4)
$\bar{d}$		2.830	$\bar{d}$		2.59

[a] Split position: I2 29.1(8)%; Cl2 70.9%. [b] Split position: I3 38.8(8)%; Cl3 61.2%. [c] Split position: I4 43.2(6)%; Cl4 56.8%. [d] Split position: I5 47.8(7)%; Cl5 52.2%. [e] Split position: I6 28.8(8)%; Cl6 71.2%. [f] Split position: I7 44.1(6)%; Cl7 55.9%. [g] Split position: I8 44.4(6)%; Cl8 55.6%

Results and Discussion

When exploratory reactions in mixed-halide zirconium cluster systems were conducted, the title phase was observed in the powder patterns of many of these reaction products.[9,11] The structure of this phase, which always forms multiply twinned crystals, has been established for the composition $[(Zr_6B)Cl_{6.44(7)}I_{6.56}]$.

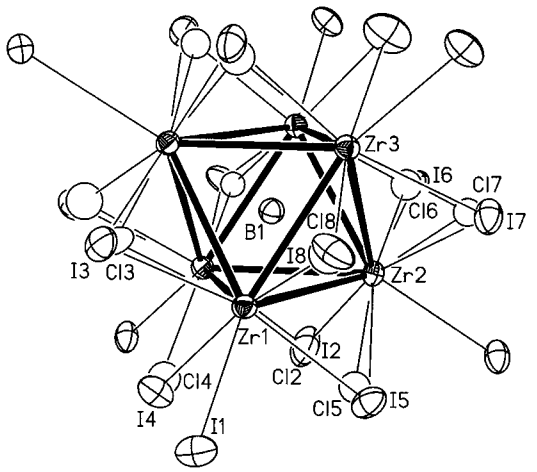

Figure 2. View of the $[(Zr_6B)I1_6{}^{a-a-a}(Cl2)_2{}^{i-i}(I,Cl)_{10}{}^{i}]$ clusters in crystals of $[(Zr_6B)Cl_{6.44(7)}I_{6.56}]$ (70% probability thermal ellipsoids) with the Zr−Zr bonds emphasized.

The structure of the title phase is composed of $[(Zr_6Z)X^i{}_{12}]$ octahedral building blocks and is similar to previously observed reduced zirconium halide octahedra containing boron as an interstitial atom. An additional six halides, X^a, are bonded to the octahedral vertexes. A displacement ellipsoid plot of the $[(Zr_6B)(Cl,I)_{18}]$ unit is shown in Figure 2 with the atom numbering scheme. Each exo position is filled by iodine atoms (I1) that are shared simultaneously by three surrounding clusters. Additional intercluster connectivity is achieved via Cl^{i-i} halides that are four-bonded in a planar fashion between two opposite edges of two neighboring (Zr_6B) octahedra. Thus, the three-dimensional connectivity can be described as $[(Zr_6B)X_{10}{}^{i}I_{6/3}{}^{a-a-a}Cl_{2/2}{}^{i-i}]$. The title phase represents a new, second structure type for this connectivity as well as for the $[(Zr_6Z)X_{13}]$ family of compounds. The previously observed structure type in the $Zr_6X_{13}Z$ family has been found in only three phases: $[(Zr_6B)Cl_{13}]$, $K[(Zr_6Be)Cl_{13}]$ (both orthorhombic), and $[(Zr_6B)Cl_{13-x}I_x]$ (tetragonal, $0 \le x \le 1.6$, structure refined for $x = 1.53(2)$).[3,10,15] All these phases contain linear chains of clusters that are connected by Cl^{i-i} that are further interconnected by three-bonded Cl^{a-a-a} atoms. Iodine substitution in the latter phase occurs only on noninterconnecting halide sites.

The new feature of the title phase is that the Cl^{i-i} atoms do not bridge opposite edges of each metal octahedron. The manner in which the two Cl^{i-i} atoms of each cluster is related to each other can be described by assuming an idealized trigonal antiprismatic Zr_6 unit with one $\bar{3}$ axis perpendicular to the two Zr triangles with the two Cl^{i-i} atoms above and below the antiprism. Applying once a (clockwise) $\bar{3}$ symmetry operation on the Cl^{i-i} halide that bridges one of the three edges of the upper Zr triangle will give the second (idealized) Cl^{i-i} position bridging the lower Zr triangle.[16] Considering only the Cl^{i-i} connectivity, zigzag chains of clusters result that run along [001] (horizontally in Figure 3). These chains are interconnected three-dimensionally by the I^{a-a-a} atoms as shown also in Figure 3. Aside from the above-mentioned $[(Zr_6Z)X_{13}]$ phases, the only other structures with these uncommon X^{i-i} bridging halides are found in the reduced rare-earth (RE) metal halide motifs $[(RE_6Z)X_{10}]$ (with RE = Y, La, or Pr; X = I or Br; Z = group 7 or 8 metals)[17−19] and $[(RE_{12}Z_2)I_{17}]$ (with RE = Pr, La, or Ce; Z = Re, Fe)[22,23] for iodine bridges and in some condensed cluster chains.[24] Such bromide bridges are found in $[(La_6Os)_8Br_{81}]$, which exhibits, besides Br^{i-i} functions, Br^{i-a-a}

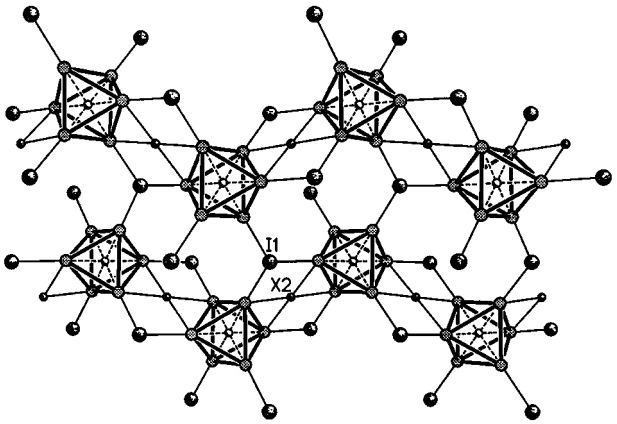

Figure 3. View of the intercluster connectivity in the $[(Zr_6B)Cl_{11-x}I_{2+x}]$ structure (*c* run horizontally). The Zr−Zr bonds are emphasized, and the *inner* halides are omitted for clarity.

functions and very uncommon face-bridging Br^{f-a} functions.[30] In zirconium halides, the unusual X^{a-a-a} functionality is observed only in the cubic $A^{I,II}[(Zr_6B)Cl_{12-x}I_{2+x}]$ ($[Nb_6I_{12-x}Cl_{2+x}]$) structure.[11,12,25] The I1 site, which exhibits the X^{a-a-a} connectivity, is solely occupied by iodine. The observation that the intercluster connecting sites can be occupied by only one type of halogen is consistent with that of the other structurally characterized mixed-halide zirconium cluster phases. In contrast, the Cl^{i-i} site shows in the refinement a small admixture of iodine (I2: 29.1(8)%) and chlorine (Cl2: 70.9%). Thus, this might be the first example of zirconium halides that contain iodine on a site with *inner*−*inner* connectivity. Unfortunately it cannot be ruled out completely at the present stage that the amount of I on the X2 site is affected by the twinning. Further experimental work seems necessary in order to verify the mixed occupation of this cluster connecting halide site. In all of the other cases of cluster interconnecting halides the Zr−X−Zr distances determine which halogen may solely occupy that site. For example, in $Na[(Zr_6B)Cl_{10.94(1)}I_{3.06}]$ the intercluster connecting I^{a-a-a} atoms have Zr−I distances of 3.194(1) Å, a value that is too long for favorable Zr−Cl bonding even for three-coordinate Cl atoms. Thus far, substitutional disorder has been only observed for *inner* halide sites with the chlorine atoms having shorter Zr−X distances than the larger iodine atoms. In a bonding situation where the Zr−X distance reaches the upper limit for a reasonable Zr−Cl bond length and the lower limit for a reasonable Zr−I bond length, mixed Cl/I sites may occur for intercluster halide bridges. This is what appears to be the case for the halide site 2 (Cl2/I2) in the present structure. The average Zr−Cl2 distance (2.802(1) Å) may be considered long but not out of range for a four-coordinate chlorine atom when compared with the Zr−Cl^{i-i} distance of 2.708(1) Å or with the Zr−Cl^{a-a-a} distance of 2.774(1) Å in $[(Zr_6B)Cl_{11.47(2)}I_{1.53}]$.[10] In a converse fashion, this Zr−I^{i-i} distance is as short as the Zr−I^{i} distances, which range between 2.77 and 2.86 Å in $Na[(Zr_6B)Cl_{10.94(1)}I_{3.06}]$[11,12] or $[(Zr_6B)Cl_{11.47(2)}I_{1.53}]$.[10] It is also important to note that the displacement parameters of the (I2/Cl2) site are not extraordinarily elongated perpendicular to the (X2, Zr_4) plane, which would result in a dumbbell-like atom arrangement with the iodine atoms occupying the outer and the Cl atoms the inner parts of the dumbbell.

Furthermore, the importance of repulsive forces between proximal halide atoms (especially iodine; matrix effects) and the relief of such X···X crowding by substitution of iodine by chlorine has been discussed in ref 10. For the cubic $Na[(Zr_6B)Cl_{2+x}I_{12-x}]$ phase it has been shown that such nonbonding halide interactions may even force *inner* chloride positions to be completely free of the iodide admixture because of otherwise too short I···I contacts.[11,12] Thus, this structure type only exists if both the iodine atoms for the I^{a-a-a} sites and Cl atoms for the *inner* halide sites are present. A similar explanation accounts for the X^{i-i} (I2, Cl2) site of the title phase. An occupation with only iodine would require much longer Zr−I distances (by ∼0.4 Å), which would force an expansion of the structure with much longer unfavorable Zr−I^{a-a-a} distances. On the other hand, an occupation with only chlorine would result in an unfavorable squeezed structure. It appears as if the combination of iodine AND chlorine on this site behaves overall as a halogen atom with the average size of both. Therefore, this "atom" fits into a structure such that the most stable (under the chosen reaction conditions) three-dimensional arrangement is formed. Exploratory reactions with bromides seem to be interesting with respect to this observation. Furthermore, a rough correlation is observed for the Zr−X2 distance with the amount of iodine admixture (i.e., 2.7 Å is correlated with 100% Cl; 3.1 Å is correlated with 100% I). This correlation indicates a value close to that refined from the X-ray data of ∼30% I occupation (see Table 4).

The remaining halide sites, X3 through X8, constitute the X^{i} functionalities. They are all occupied statistically with a mixture of chlorine and iodine. All these sites are positionally resolved in the X-ray structure. The Zr−Cl^{i} distances range between 2.48 and 2.66 Å, similar to those found in other structurally characterized chloride−iodide−zirconium cluster phases.[10−12] The Zr−I^{i} distances average to 2.830 Å, compared to 2.853 Å in $[(Zr_6B)Cl_{1.65}I_{10.55}]$[10] or 2.858 Å in $[(Zr_6B)Cl_{11.47}I_{1.53}]$. The distances within the (Zr_6B) unit compare well with those of other reduced zirconium boride halides. The average Zr−Zr distance of 3.299 Å and the Zr−B distance of 2.335 Å attest for the interstitial being boron because these distances depend strongly on the type of the interstitial present. The average Zr−$I1^{a-a-a}$ distance of 3.106 Å is slightly shorter than the comparable distance of the three-coordinate iodine atom in $Na[(Zr_6B)Cl_{10.94(1)}I_{3.06}]$ (3.194(1) Å) and $Sr_{0.5}[(Zr_6B)Cl_{10.94(1)}I_{3.06}]$ (3.182(1) Å).[12]

As is visible from Figure 2, the only symmetry elements involved in the cluster unit is a 2-fold axis, passing through I3 (Cl3), B1, and I6 (Cl6), and inversion centers at the X2 position. The two-coordinate *inner* halide sites X3 through X8 are substitutionally disordered with iodine and chlorine. Inspection of nonbonding iodine···iodine contacts shows that distances below the critical value of ∼3.9 Å exist. This indicates that some sort of ordering must exist to avoid repulsive contacts. Such an ordering is only possible if each site has less than 50% iodine admixture, which is in fact observed in the X-ray structure (see Table 4). However, no superstructure reflections were observed in the X-ray diffraction data.

The phase width was deduced from the products of the reactions that are listed in Table 1. Reaction numbers 1−12 are given with decreasing I/Cl ratio of the starting materials. The $[(Zr_6B)Cl_{11-x}I_{2+x}]$ phase forms at I/Cl ratios between ∼1.6 and ∼0.18. This corresponds to about $0 \le x \le 6$. All these reactions were run between 800 and 850 °C. Lower temperatures give only small yields or different phases, as is visible from reaction numbers 13−17. Entries 18 and 19 with Mg- and La-containing starting materials resulted in simple Mg and La salts and the title phase. Thus, if such cations cannot be incorporated in a cluster phase, a cation-free phase, i.e., the title phase, forms from material left from the separation of the simple salt. The last two entries, reactions run with Be as the interstitial but without an alkaline cation, did not give the title phase with a

cluster electron count of 13. The $[(Zr_6Z)X_{12}]$ structure was formed instead.

Table 2 gives lattice parameters and unit cell volumes of some members of the $[(Zr_6B)Cl_{11-x}I_{2+x}]$ phase with different I/Cl ratios of the starting materials. These values were obtained from refining of the positions of indexed lines on Guinier diagrams. Because of the formation of side products (if any), the I/Cl ratio in the final $[(Zr_6B)Cl_{11-x}I_{2+x}]$ compound may be different from the I/Cl ratio of the starting materials (see, for example, the $Zr_6Cl_5I_8B$ entry run at 800 °C in Table 2). Therefore, the cell volumes cannot be directly correlated with the I/Cl ratios. Anyhow, with increasing iodine content, the cell volumes increase, as expected. Some small variations of about 1.5% are observed in the cell volumes from reaction products with the same I/Cl ratio but run at different temperature.

The results from the synthesis and characterization of the $[(Zr_6B)Cl_{11-x}I_{2+x}]$ phase as well as of the cubic $A^{I,II}[(Zr_6B)Cl_{2+x}I_{12-x}]$[11,12] phase show that for the understanding of structures and stabilities of zirconium cluster phases (and others) not only factors like metal−metal bonding and metal−interstitial bonding but also the size of the anions (van der Waals contacts) play a crucial role. The best match of all of these parameters finally determines which structure is formed.

Acknowledgment. This work was supported by the Deutsche Forschungsgemeinschaft (DFG) through a postdoctoral fellowship (M.K. 1995−1997) and the University of Duisburg/Germany. We are grateful to Prof. Dr. G. Henkel (University of Duisburg/Germany), Prof. J. D. Corbett (Iowa State University, Ames, IA), Prof. Dr. A. Mewis, Dr. H. Wunderlich (University of Düsseldorf/Germany), and Dr. G. Kreiner (University of Dortmund/Germany) for valuable discussions and support, and we thank Dr. G. F. Höfer (Heraeus Quarzglas GmbH), M. Barros (NPC GmbH), Dr. L. Häming, and Dr. M. Ruf (Bruker axs) for technical support. We also thank Dr. R.-Y. Qi for sharing preliminary observations of the mixed-halide zirconium cluster chemistry with us.

Supporting Information Available: Tables listing detailed crystallographic data, atomic positional parameters, and bond lengths and angles; and one X-ray crystallographic file, in CIF format. This material is available free of charge via the Internet at http://pubs.acs.org.

IC991359V